

## Long-living prethermalization in nearly integrable spin ladders

J. Pawłowski<sup>1</sup>, M. Panfil<sup>2</sup>, J. Herbrych<sup>1</sup> and M. Mierzejewski<sup>1</sup>

<sup>1</sup>*Institute of Theoretical Physics, Faculty of Fundamental Problems of Technology,  
Wrocław University of Science and Technology, 50-370 Wrocław, Poland*

<sup>2</sup>*Faculty of Physics, University of Warsaw, Pasteura 5, 02-093 Warsaw, Poland*



(Received 18 December 2023; revised 18 March 2024; accepted 1 April 2024; published 17 April 2024)

Relaxation rates in nearly integrable systems usually increase quadratically with the strength of the perturbation that breaks integrability. We show that the relaxation rates can be significantly smaller in systems that are integrable along two intersecting lines in the parameter space. In the vicinity of the intersection point, the relaxation rates of certain observables increase with the fourth power of the distance from this point, whereas for other observables one observes standard quadratic dependence on the perturbation. As a result, one obtains exceedingly long-living prethermalization but with a reduced number of the nearly conserved operators. We show also that such a scenario can be realized in spin ladders.

DOI: [10.1103/PhysRevB.109.L161109](https://doi.org/10.1103/PhysRevB.109.L161109)

*Introduction.* The time evolution of generic quantum systems tends towards the thermal equilibrium [1–5] independently of the initial state. In recent years, systems in which thermalization occurs very slowly [6] or can be completely eliminated [7] have attracted a lot of interest. Particular attention was paid to integrable systems which avoid thermalization and evolve towards a generalized Gibbs state [8–12]. The crucial role in the behavior of such systems is played by local (or quasilocal) integrals of motion (LIOMs) whose presence prevents thermalization of local observables [13,14] and has important consequences for the transport properties of integrable systems [15–18]. However, more realistic models as well as experimental setups contain small, but non-negligible, perturbations which break the integrability [19–25]. While one expects that the asymptotic dynamics of such nearly integrable (NI) systems is diffusive [26–28], the dynamics at intermediate timescales resembles that of integrable models. The latter transient dynamics of NI systems is known as prethermalization [29–32].

A particularly important example of the integrability breaking occurs in systems of weakly coupled integrable chains [6,33]. While the interchain coupling can be well controlled in the cold-atom experiments [34], it is not always possible to completely eliminate this interaction [35]. Quite obviously, a nonvanishing interchain coupling is unavoidable in solid-state systems [36,37]. Moreover, recent quasiclassical studies based on the Boltzmann collision integral approach [38,39] indicate that extremely long relaxation times may occur in such NI systems.

It is rather obvious that one is most interested in NI systems in which the relaxation times are as long as possible. While an NI system may host very distinct relaxation times [32,40–42], the corresponding relaxation rates typically scale quadratically with the strength of the integrability-breaking perturbation [21,22,40,42,43]. Under such a scenario, the only way to increase the relaxation times is to reduce the perturbation. In this Letter, we establish another possibility of decreasing the relaxation rates in NI systems. Namely, we consider a

system that is integrable along two intersecting lines in the parameter space (see, e.g., Refs. [44–46] for an example of such systems). If certain LIOMs on both lines have large overlaps, then the corresponding relaxation rates increase with the fourth power of the distance (in the parameter space) from the intersection point. Relaxation rates for LIOMs that do not have such overlaps exhibit standard quadratic dependence on the perturbation. As a consequence, extremely small relaxation rates and arbitrary larger ratios of relaxation times appear in the studied NI system. Finally, we show that such a scenario can be implemented in nearly integrable spin ladders introduced below.

*Spin ladder.* We investigate a spin ladder consisting of two XXZ chains coupled via anisotropic spin-spin interaction of strength  $U$ :

$$H = \sum_{\ell=1}^2 H_{\ell} + U \sum_{j=1}^L S_{j,1}^z S_{j,2}^z, \quad (1)$$

$$H_{\ell} = \frac{J}{2} \sum_{j=1}^L (S_{j,\ell}^+ S_{j+1,\ell}^- + \text{H.c.}) + \Delta \sum_{j=1}^L S_{j,\ell}^z S_{j+1,\ell}^z. \quad (2)$$

The subscripts  $\ell = 1$  and  $2$  and  $j = 1, \dots, L$  denote, respectively, the leg and the site within a leg on which the spin-1/2 operators act. From now on we set  $J = 1$ , fix the total magnetization to  $S_{\text{tot}}^z = 0$ , and assume periodic boundary conditions along the legs of the ladder.

The ladder is shown schematically in Fig. 1(a). It is integrable for  $U = 0$  and inherits a complete set of LIOMs  $\{Q_{n,1}\}$  and  $\{Q_{n,2}\}$  from both XXZ chains. In this work we use analytic forms of LIOMs and the notation from Ref. [47]. In particular,  $Q_{1,\ell}$  and  $Q_{2,\ell}$  denote respectively the total magnetization and the Hamiltonians of the chain  $\ell$ . Here, we focus on the dynamics of the first two nontrivial XXZ LIOMs, namely,  $Q_{3,\ell}$  and  $Q_{4,\ell}$ , supported on three and four sites, respectively. This choice is motivated by the fact that  $Q_{3,\ell}$  is the energy current and thus it is an experimentally relevant quantity. In order to

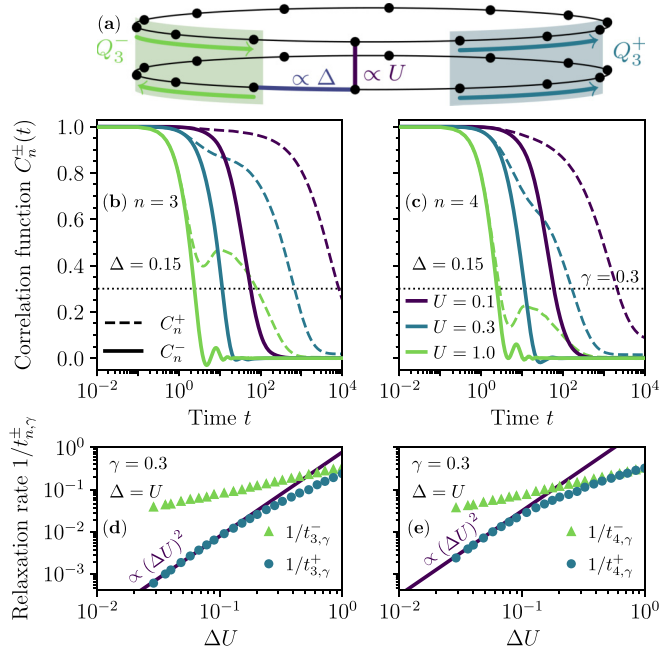


FIG. 1. (a) Sketch of the ladder in Eq. (1) with marked  $S^z$ - $S^z$  interactions ( $\Delta, U$ ) and nearly conserved operators ( $Q_n^\pm$ ). (b,c) Correlation functions  $C_n^\pm(t)$  defined in Eq. (3) obtained for a ladder with  $L = 14$  rungs. (b) Dashed and continuous curves show  $C_3^+(t)$  and  $C_3^-(t)$ , respectively. (c) The same as in panel (b) but for  $C_4^\pm(t)$ . Horizontal dotted lines in panels (b) and (c) define times,  $t_{n,\gamma}^\pm$ , when  $C_n^\pm(t_{n,\gamma}^\pm) = \gamma = 0.3$ . The legends in panels (b) and (c) are common for both panels. Panels (d) and (e) show  $1/t_{3,\gamma}^\pm$  and  $1/t_{4,\gamma}^\pm$  for NI systems with  $U = \Delta$  and  $\gamma = 0.3$  (see text for details).

demonstrate that the discussed properties are not unique to just a single quantity, we study also  $Q_{4,\ell}$ .

It is convenient to introduce symmetrized combinations of the latter LIOMs,  $Q_n^\pm \equiv Q_{n,1} \pm Q_{n,2}$ . In the case of uncoupled chains,  $Q_n^+$  and  $Q_n^-$  are strictly conserved and thus the correlation functions are time independent, i.e.,  $\langle Q_n^\pm(t) Q_n^\pm \rangle = \text{const}$ , and we use a simplified notation  $Q_n^\pm \equiv Q_n^\pm(t=0)$ . However, the interaction term  $U \neq 0$  breaks the integrability of the studied model so that  $\langle Q_n^\pm(t) Q_n^\pm \rangle$  decay in time. In the following we show that the sums of the XXZ LIOMs,  $Q_n^+$ , decay much slower than their differences,  $Q_n^-$ . We present an explanation of this unexpected behavior, by inspecting a dual point of view, in which the intrachain term  $\propto \Delta$  is also treated as an integrability-breaking perturbation. Namely, for  $\Delta = 0$ , the Hamiltonian of the ladder reduces to the Hubbard chain, in which the leg index  $\ell$  labels the spin projection of fermions. This view introduces another set of LIOMs  $\{I_n\}$ , originating from the integrability of the Hubbard chain. Here, we argue that the decay of  $Q_n^+$  or  $I_n$  in the NI model ( $U \neq 0, \Delta \neq 0$ ) is significantly slowed down due to large overlaps of both sets of LIOMs.

*Dynamics of nearly conserved observables.* To probe the dynamics of the nearly integrable spin ladder, we calculate the real-time correlation functions

$$C_n^\pm(t) = \langle e^{iHt} Q_n^\pm e^{-iHt} Q_n^\pm \rangle. \quad (3)$$

Here,  $\langle AB \rangle = \frac{1}{\mathcal{Z}} \text{Tr}(AB)$  is the Hilbert-Schmidt inner product for Hermitian operators  $A$  and  $B$ , and  $\mathcal{Z} = \text{Tr}(\mathbb{1})$  is the

dimension of the Hilbert space. We recall that the Hilbert-Schmidt product is mathematically equivalent to the ensemble average at infinite temperature.

We note that  $Q_{4,\ell}$  and  $I_4$  in Ref. [47] are not orthogonal to the respective integrable Hamiltonians,  $H_\ell$  and  $H(\Delta = 0)$ . Therefore, we first subtract their projections on the Hamiltonians and obtain orthogonal sets of LIOMs. All considered LIOMs are also Hilbert-Schmidt normalized, i.e.,  $\|Q_n^\pm\|^2 = \langle Q_n^\pm Q_n^\pm \rangle = 1$ , and thus the correlation functions in Eq. (3) are equal to 1 at  $t = 0$ . We refer to the Supplemental Material [48] for explicit forms of LIOMs and their overlaps.

Utilizing the Lanczos time-evolution method [52,53] combined with the dynamical typicality [54–58], we calculate correlation functions introduced in Eq. (3); see Ref. [48] for the details of numerical calculations. Figures 1(b) and 1(c) show, respectively,  $C_3^\pm(t)$  and  $C_4^\pm(t)$  calculated for small anisotropy  $\Delta = 0.15$  and different strengths of the interchain interaction,  $U = 0.1, 0.3$ , and  $1$ . In the regime of small  $U$  one observes that the correlation functions obtained for  $Q_n^+$  (dashed lines) decay much slower than the correlation functions determined for  $Q_n^-$  (continuous lines). In the Supplemental Material [48] we show that the differences between  $C_n^+(t)$  and  $C_n^-(t)$  become significant for much shorter times than the timescale at which  $C_n^+(t)$  develops the finite-size effects. Therefore, the exceedingly different relaxation times for  $Q_n^+$  and  $Q_n^-$  do not emerge as finite-size artifacts.

In order to capture the differences between relaxation of  $Q_n^+$  and  $Q_n^-$  in a quantitative manner, we determine times when the correlation functions decay to a fraction of  $\gamma$  of their initial value, such that  $C_n^\pm(t_{n,\gamma}^\pm) = \gamma$  [see dotted lines in Figs. 1(b) and 1(c)]. While the accessible system sizes do not allow us to reliably establish the true relaxation rates, we assume that their dependence on  $U$  and  $\Delta$  can be estimated from  $t_{n,\gamma}^\pm$ . In Figs. 1(d) and 1(e) we show the corresponding relaxation rates  $1/t_{3,\gamma}^\pm$  and  $1/t_{4,\gamma}^\pm$  for a NI system along the line  $U = \Delta$  where we set  $\gamma = 0.3$ . In the regime of weak interactions, one observes that the relaxation rates for  $Q_n^+$  increase only as  $U^2 \Delta^2$ ; i.e., they are much smaller than the squared strengths of integrability-breaking interactions  $U^2$  or  $\Delta^2$ . However, the relaxation rates for the other set of nearly conserved operators,  $Q_n^-$ , show much weaker dependence on perturbations and may be larger than  $1/t_{n,\gamma}^+$  by a few orders of magnitude.

Next we check how the differences between  $t_{n,\gamma}^+$  and  $t_{n,\gamma}^-$  depend on the parameters of the studied model. To this end we calculate the ratio  $R_n(\gamma) = (t_{n,\gamma}^+ - t_{n,\gamma}^-)/(t_{n,\gamma}^+ + t_{n,\gamma}^-)$ . Numerical results for this ratio are shown in Fig. 2 on an evenly spaced rectangular grid in the parameter space  $(\Delta, U)$ . Blank parts on the plots correspond to the situation when  $t_n^+$  is larger than the longest time accessible in our numerical calculations,  $t \sim 10^4$ . For small  $\Delta$  and  $U$ , we observe that  $R_n(\gamma)$  is close to 1 for both  $n = 3$  and  $n = 4$ . This means that the decay times for  $Q_n^-$  are negligibly small when compared to the timescale that corresponds to the slow relaxation of  $Q_n^+$ . For large  $\Delta$  and  $U$ , we observe that  $Q_n^+$  and  $Q_n^-$  relax rather quickly and with roughly the same relaxation times,  $t_{n,\gamma}^+ \simeq t_{n,\gamma}^-$ .

*Significance of overlapping LIOMs.* In order to explain the origin of the exceedingly different and long relaxation times, we turn to a dual picture. Namely, we consider the anisotropy term ( $\sim \Delta$ ) as a perturbation to the integrable Hubbard chain

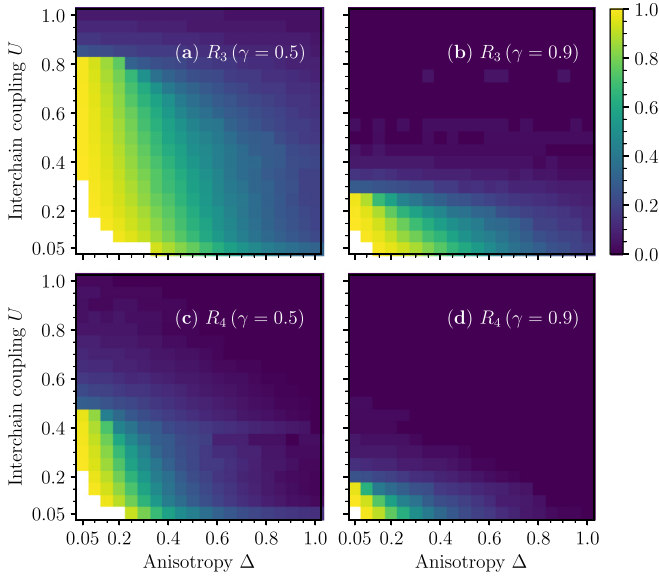


FIG. 2. Ratio  $R_n(\gamma)$  calculated for  $L = 12$ . Blank regions correspond to parameters for which  $C_n^+(t) > \gamma$  for the numerically accessible times  $t \sim 10^4$ , e.g., see  $C_n^+(t)$  for  $U = 0.1$  in Fig. 1(b).

described by the Hamiltonian  $H(\Delta = 0)$ . The latter Hamiltonian possesses another complete set of LIOMs  $\{I_n\}$ . In what follows, we demonstrate that the slower decay of the operators  $Q_n^+$  in the nearly integrable ladder ( $\Delta \neq 0$  and  $U \neq 0$ ) can be linked to their substantial overlaps with  $I_n$ . Such overlaps do not exist for the quickly decaying operators  $Q_n^-$ . We note that  $Q_n^-$  operators are odd under the spin-flip transformation,  $\ell \rightarrow 3 - \ell$ , whereas the Hubbard LIOMs,  $I_n$ , are even under such spin-flip so that one obtains  $\langle Q_n^- I_n \rangle = 0$ .

In Fig. 3 we present the overlaps  $\langle Q_n^+ I_n \rangle$ . In order to completely eliminate the finite-size effects, the overlaps were calculated analytically in the full Hilbert space that includes all of the  $S_{\text{tot}}^z$  sector. In particular, one finds

$$\langle Q_3^+ I_3 \rangle = \frac{J^2}{\sqrt{(J^2 + 2U^2)(J^2 + 2\Delta^2)}}, \quad (4)$$

and the explicit form of the other overlap  $\langle Q_4^+ I_4 \rangle$  is shown in Ref. [48]. We have also checked that the numerically obtained overlaps in the sector with  $S_{\text{tot}}^z = 0$  (not shown) are

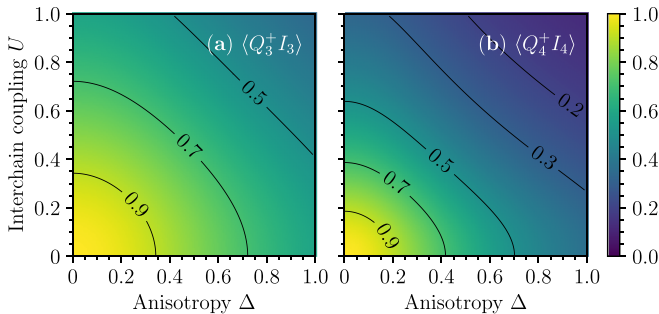


FIG. 3. Overlaps  $\langle Q_n^+ I_n \rangle$  calculated analytically for  $L \rightarrow \infty$ , see Eq. (4) and Ref. [48] for more details. Black solid curves are isolines. Note that  $Q_n^+$  and  $I_n$  are strictly conserved for  $U = 0$  and  $\Delta = 0$ , respectively.

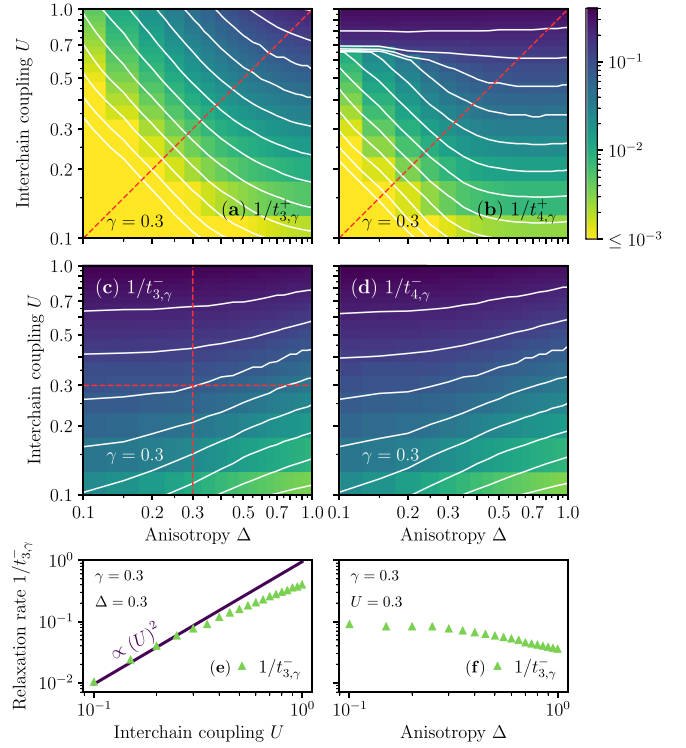


FIG. 4. (a)–(d) Relaxation rates  $1/t_{n,\gamma}^\pm$  estimated from the correlation functions in Eq. (3) via relation  $C_n^\pm(t_{n,\gamma}^\pm) = \gamma$  for  $\gamma = 0.3$  and  $L = 12$ . Continuous curves represent isolines. Dashed lines in panels (a) and (b) mark parameters for which relaxation rates are shown in Figs. 1(d) and 1(e). Panels (e) and (f) show relaxation rates  $1/t_{n,\gamma}^-$  along the dashed lines marked in panel (c).

qualitatively the same as the results in Fig. 3. Comparing Fig. 2 with Fig. 3, we find that the differences in relaxations of  $Q_n^+$  and  $Q_n^-$  are most pronounced for the same parameters where the overlaps  $\langle Q_n^+ I_n \rangle$  are large.

Finally, we establish a simple link between the overlaps of LIOMs of integrable models ( $U = 0$  or  $\Delta = 0$ ) and the slow dynamics of  $Q_n^+$  in the nearly integrable ladder with ( $U \neq 0$  and  $\Delta \neq 0$ ). To this end we conjecture that in the regime of small  $U$  and  $\Delta$ , the relaxation rates for  $Q_n^+$  and  $Q_n^-$  can be expanded in powers of  $\Delta^2$  and  $U^2$ . Since  $Q_n^-$  are strictly conserved only for  $U = 0$  and arbitrary  $\Delta$ , the lowest-order contributions to their relaxation rates are  $1/t_{n,\gamma}^- \propto U^2$ , as it is expected for a generic integrability-breaking perturbation. However, due to large overlaps  $\langle Q_n^+ I_n \rangle$ , the relaxation rates for  $Q_n^+$  vanish for both  $U = 0$  and  $\Delta = 0$ . Therefore, these relaxation rates cannot contain terms which depend solely on either  $U$  or  $\Delta$ , and thus the lowest-order contributions are  $1/t_{n,\gamma}^+ \propto \Delta^2 U^2$ . Consequently, for small  $\Delta$ , one obtains  $t_{n,\gamma}^+ \gg t_{n,\gamma}^-$ .

This scenario is clearly confirmed by the results in Figs. 4(a) and 4(b). In these plots we show heat maps for  $1/t_{n,\gamma}^+$  using logarithmic scales for  $U$  and  $\Delta$ . One observes that the isolines roughly follow straight lines consistent with the dependence  $1/t_{n,\gamma}^+ \propto (\Delta U)^\alpha = \text{const}$ . Numerical results obtained in a direction that is perpendicular to the isolines ( $U = \Delta$ ) are shown in Figs. 1(d) and 1(e), demonstrating that the exponent  $\alpha = 2$ . Using parametrizations  $U = d \cos(\phi)$

and  $\Delta = d \sin(\phi)$ , we find that the relaxation rate for  $Q_n^+$  grows as  $d^4$ . Here,  $d$  is the distance from the intersection of two lines,  $\Delta = 0$  and  $U = 0$ , along which the studied model is integrable.

In the case of  $1/t_n^-$ , one observes very different isolines with positive slopes [see Figs. 4(c) and 4(d)]. The latter are consistent with the conjecture that  $1/t_{n,\gamma}^-$  are determined mostly by the interchain interaction  $U$ . For the sake of completeness we have calculated  $1/t_{n,\gamma}^-$  in the directions that are roughly perpendicular or parallel to the corresponding isolines, i.e., for  $\Delta = \text{const}$  or  $U = \text{const}$ . Numerical results shown in Figs. 4(e) and 4(f) confirm the standard quadratic dependence of  $1/t_{n,\gamma}^-$  on the perturbation  $U$ .

Since the proximity of two integrable lines is responsible for the long-living prethermalization in the studied ladder, one may expect to find a broader class of operators which exhibit slow relaxation. In the Supplemental Material [48] we show that linear combinations of  $Q_n^+$  and  $I_n$  show very similar dynamics. As expected, breaking of integrability along one of the lines (e.g., via other forms of the coupling between the legs) destroys the exceptional properties of the studied system [48].

**Conclusions.** We have considered a ladder consisting of two XXZ chains (each with spin anisotropy  $\Delta$ ) coupled via interaction of strength  $U$ . The studied model is integrable along two lines in the parameter space. Namely, for  $\Delta = 0$  the ladder represents the Hubbard chain with one set of LIOMs  $\{I_n\}$ , whereas for  $U = 0$  one obtains two uncoupled XXZ chains. In the latter case we have introduced LIOMs which are symmetric,  $\{Q_n^+\}$ , or antisymmetric,  $\{Q_n^-\}$ , with respect to exchanging the chains. Studying the dynamics of a nearly integrable ladder with ( $U \neq 0$  and  $\Delta \neq 0$ ) we have found that correlation functions for  $Q_n^+$  decay much slower than those for  $Q_n^-$  and that the difference of relaxation times is most pronounced for small  $U$  and  $\Delta$ .

We have linked this result with large overlaps between  $Q_n^+$  and  $I_n$  and vanishing overlaps between  $Q_n^-$  and  $I_n$ . As a consequence of the former overlaps, the relaxation rates for  $Q_n^+$  must vanish for both  $U = 0$  and  $\Delta = 0$ , so that the lowest-order contribution to the relaxation rates is at most of the order of  $\Delta^2 U^2$ . In contrast to this, the relaxation rates for  $Q_n^-$  are of the order of  $U^2$ . Such behavior explains exceedingly different

relaxation times observed for  $Q_n^+$  and  $Q_n^-$  in the regime of small  $U$  and  $\Delta$ . Consequently, in this regime of parameters one deals with a rather specific prethermalization. Namely, the number of nearly conserved quantities,  $Q_n^+$ , is twice smaller than the number of LIOMs in the uncoupled chains, where both  $Q_n^+$  and  $Q_n^-$  are conserved.

These findings can be further examined from the point of view of quasiclassical analysis based on the Boltzmann collision integral [38,49] (see also Refs. [32,41] for the hydrodynamic perspective on the integrability breaking). The central assumption here is that each leg of the spin chain is in a state described by the generalized Gibbs ensemble (GGE) of the XXZ spin chain [50]. The whole system is then in the product state of the two GGE states. The coupling between the legs leads then, by Fermi's golden rule, to an evolution of states of each leg. As we show in the Supplemental Material [48], both families of charges  $Q_n^\pm$  are conserved during this evolution up to order  $\Delta^2 U^2$  in a case when the anisotropy parameters and the states of the two legs are identical. Otherwise,  $Q_n^-$  may acquire dynamics at lower orders while  $Q_n^+$  does not. Our results reinforce this quasiclassical picture.

Our reasoning is general and is expected to hold true also for other systems which are integrable along two intersecting lines in the parameter space. However, this should be verified by direct calculations. The essential condition is that the LIOMs on both integrable lines have large mutual overlaps in the vicinity of the crossing point. Then, in the vicinity of this point one may expect long-living prethermalization with relaxation rates that increase with the fourth power of the distance in the parameter space from the intersection point. This is in contrast to the case of generic nearly integrable systems where relaxation rates increase with the second power of the perturbation. The long-living prethermalization in the studied ladder leads to a very slow relaxation of the energy current [48] that should also be visible as a high thermal conductivity.

**Acknowledgments.** M.M. and J.P. acknowledge support by the National Science Centre (NCN), Poland, via Project No. 2020/37/B/ST3/00020. M.P. acknowledges support by the National Science Centre (NCN), Poland, via Project No. 2022/47/B/ST2/03334. Part of the calculations has been carried out using resources provided by Wroclaw Centre for Networking and Supercomputing [59].

- 
- [1] S. Trotzky, Y.-A. Chen, A. Flesch, I. P. McCulloch, U. Schollwöck, J. Eisert, and I. Bloch, Probing the relaxation towards equilibrium in an isolated strongly correlated 1D Bose gas, *Nat. Phys.* **8**, 325 (2012).
- [2] A. M. Kaufman, M. E. Tai, A. Lukin, M. Rispoli, R. Schittko, P. M. Preiss, and M. Greiner, Quantum thermalization through entanglement in an isolated many-body system, *Science* **353**, 794 (2016).
- [3] C. Neill, P. Roushan, M. Fang, Y. Chen, M. Kolodrubetz, Z. Chen, A. Megrant, R. Barends, B. Campbell, B. Chiaro, A. Dunsworth, E. Jeffrey, J. Kelly, J. Mutus, P. J. J. O'Malley, C. Quintana, D. Sank, A. Vainsencher, J. Wenner, T. C. White *et al.*, Ergodic dynamics and thermalization in an isolated quantum system, *Nat. Phys.* **12**, 1037 (2016).
- [4] A. P. Luca D'Alessio, Y. Kafri, and M. Rigol, From quantum chaos and eigenstate thermalization to statistical mechanics and thermodynamics, *Adv. Phys.* **65**, 239 (2016).
- [5] M. Rigol, V. Dunjko, and M. Olshanii, Thermalization and its mechanism for generic isolated quantum systems, *Nature (London)* **452**, 854 (2008).
- [6] Y. Tang, W. Kao, K.-Y. Li, S. Seo, K. Mallayya, M. Rigol, S. Gopalakrishnan, and B. L. Lev, Thermalization near integrability in a dipolar quantum Newton's cradle, *Phys. Rev. X* **8**, 021030 (2018).
- [7] T. Kinoshita, T. Wenger, and D. S. Weiss, A quantum Newton's cradle, *Nature (London)* **440**, 900 (2006).
- [8] M. Rigol, V. Dunjko, V. Yurovsky, and M. Olshanii, Relaxation in a completely integrable many-body quantum system: An

- ab initio* study of the dynamics of the highly excited states of 1D lattice hard-core bosons, *Phys. Rev. Lett.* **98**, 050405 (2007).
- [9] A. C. Cassidy, C. W. Clark, and M. Rigol, Generalized thermalization in an integrable lattice system, *Phys. Rev. Lett.* **106**, 140405 (2011).
- [10] F. Lange, Z. Lenarčič, and A. Rosch, Time-dependent generalized Gibbs ensembles in open quantum systems, *Phys. Rev. B* **97**, 165138 (2018).
- [11] E. Ilievski, J. De Nardis, B. Wouters, J.-S. Caux, F. H. L. Essler, and T. Prosen, Complete generalized Gibbs ensembles in an interacting theory, *Phys. Rev. Lett.* **115**, 157201 (2015).
- [12] T. Langen, S. Erne, R. Geiger, B. Rauer, T. Schweigler, M. Kuhnert, W. Rohringer, I. E. Mazets, T. Gasenzer, and J. Schmiedmayer, Experimental observation of a generalized Gibbs ensemble, *Science* **348**, 207 (2015).
- [13] P. Mazur, Non-ergodicity of phase functions in certain systems, *Physica* **43**, 533 (1969).
- [14] X. Zotos, F. Naef, and P. Prelovšek, Transport and conservation laws, *Phys. Rev. B* **55**, 11029 (1997).
- [15] B. Bertini, F. Heidrich-Meisner, C. Karrasch, T. Prosen, R. Steinigeweg, and M. Žnidarič, Finite-temperature transport in one-dimensional quantum lattice models, *Rev. Mod. Phys.* **93**, 025003 (2021).
- [16] B. Bertini, M. Collura, J. De Nardis, and M. Fagotti, Transport in out-of-equilibrium XXZ chains: Exact profiles of charges and currents, *Phys. Rev. Lett.* **117**, 207201 (2016).
- [17] E. Ilievski and J. De Nardis, Microscopic origin of ideal conductivity in integrable quantum models, *Phys. Rev. Lett.* **119**, 020602 (2017).
- [18] J. De Nardis, S. Gopalakrishnan, R. Vasseur, and B. Ware, Stability of superdiffusion in nearly integrable spin chains, *Phys. Rev. Lett.* **127**, 057201 (2021).
- [19] T. Prosen, Time evolution of a quantum many-body system: Transition from integrability to ergodicity in the thermodynamic limit, *Phys. Rev. Lett.* **80**, 1808 (1998).
- [20] X. Zotos, High temperature thermal conductivity of two-leg spin-1/2 ladders, *Phys. Rev. Lett.* **92**, 067202 (2004).
- [21] P. Jung, R. W. Helmes, and A. Rosch, Transport in almost integrable models: Perturbed Heisenberg chains, *Phys. Rev. Lett.* **96**, 067202 (2006).
- [22] P. Jung and A. Rosch, Spin conductivity in almost integrable spin chains, *Phys. Rev. B* **76**, 245108 (2007).
- [23] Y. Huang, C. Karrasch, and J. E. Moore, Scaling of electrical and thermal conductivities in an almost integrable chain, *Phys. Rev. B* **88**, 115126 (2013).
- [24] F. H. L. Essler, S. Kehrein, S. R. Manmana, and N. J. Robinson, Quench dynamics in a model with tuneable integrability breaking, *Phys. Rev. B* **89**, 165104 (2014).
- [25] G. P. Brandino, J.-S. Caux, and R. M. Konik, Glimmers of a quantum KAM theorem: Insights from quantum quenches in one-dimensional Bose gases, *Phys. Rev. X* **5**, 041043 (2015).
- [26] T. LeBlond, D. Sels, A. Polkovnikov, and M. Rigol, Universality in the onset of quantum chaos in many-body systems, *Phys. Rev. B* **104**, L201117 (2021).
- [27] M. Žnidarič, Weak integrability breaking: Chaos with integrability signature in coherent diffusion, *Phys. Rev. Lett.* **125**, 180605 (2020).
- [28] A. Bastianello, A. De Luca, B. Doyon, and J. De Nardis, Thermalization of a trapped one-dimensional Bose gas via diffusion, *Phys. Rev. Lett.* **125**, 240604 (2020).
- [29] M. Kollar, F. A. Wolf, and M. Eckstein, Generalized Gibbs ensemble prediction of prethermalization plateaus and their relation to nonthermal steady states in integrable systems, *Phys. Rev. B* **84**, 054304 (2011).
- [30] B. Bertini, F. H. L. Essler, S. Groha, and N. J. Robinson, Prethermalization and thermalization in models with weak integrability breaking, *Phys. Rev. Lett.* **115**, 180601 (2015).
- [31] K. Mallayya, M. Rigol, and W. De Roeck, Prethermalization and thermalization in isolated quantum systems, *Phys. Rev. X* **9**, 021027 (2019).
- [32] A. Bastianello, A. D. Luca, and R. Vasseur, Hydrodynamics of weak integrability breaking, *J. Stat. Mech.* (2021) 114003.
- [33] J.-S. Caux, B. Doyon, J. Dubail, R. Konik, and T. Yoshimura, Hydrodynamics of the interacting Bose gas in the quantum Newton cradle setup, *SciPost Phys.* **6**, 070 (2019).
- [34] P. Bordia, H. P. Lüschen, S. S. Hodgman, M. Schreiber, I. Bloch, and U. Schneider, Coupling identical one-dimensional many-body localized systems, *Phys. Rev. Lett.* **116**, 140401 (2016).
- [35] W. Kao, K.-Y. Li, K.-Y. Lin, S. Gopalakrishnan, and B. L. Lev, Topological pumping of a 1D dipolar gas into strongly correlated prethermal states, *Science* **371**, 296 (2021).
- [36] A. Scheie, N. E. Sherman, M. Dupont, S. E. Nagler, M. B. Stone, G. E. Granroth, J. E. Moore, and D. A. Tennant, Detection of Kardar-Parisi-Zhang hydrodynamics in a quantum Heisenberg spin-1/2 chain, *Nat. Phys.* **17**, 726 (2021).
- [37] W. Gannon, I. A. Zaliznyak, L. Wu, A. Feiguin, A. Tsvelik, F. Demmel, Y. Qiu, J. Copley, M. Kim, and M. Aronson, Spinon confinement and a sharp longitudinal mode in Yb<sub>2</sub>Pt<sub>2</sub>Pb in magnetic fields, *Nat. Commun.* **10**, 1123 (2019).
- [38] M. Panfil, S. Gopalakrishnan, and R. M. Konik, Thermalization of interacting quasi-one-dimensional systems, *Phys. Rev. Lett.* **130**, 030401 (2023).
- [39] M. Łebek, M. Panfil, and R. M. Konik, Prethermalization in coupled one-dimensional quantum gases, [arXiv:2303.12490](https://arxiv.org/abs/2303.12490).
- [40] M. Mierzejewski, T. Prosen, and P. Prelovšek, Approximate conservation laws in perturbed integrable lattice models, *Phys. Rev. B* **92**, 195121 (2015).
- [41] A. J. Friedman, S. Gopalakrishnan, and R. Vasseur, Diffusive hydrodynamics from integrability breaking, *Phys. Rev. B* **101**, 180302(R) (2020).
- [42] M. Mierzejewski, J. Pawłowski, P. Prelovšek, and J. Herbrych, Multiple relaxation times in perturbed XXZ chain, *SciPost Phys.* **13**, 013 (2022).
- [43] K. Mallayya and M. Rigol, Quantum quenches and relaxation dynamics in the thermodynamic limit, *Phys. Rev. Lett.* **120**, 070603 (2018).
- [44] G. Delfino, P. Grinza, and G. Mussardo, Decay of particles above threshold in the Ising field theory with magnetic field, *Nucl. Phys. B* **737**, 291 (2006).
- [45] M. Kormos, M. Collura, G. Takács, and P. Calabrese, Real-time confinement following a quantum quench to a non-integrable model, *Nat. Phys.* **13**, 246 (2017).
- [46] T. Fogarty, M. Á. García-March, L. F. Santos, and N. L. Harshman, Probing the edge between integrability and quantum chaos in interacting few-atom systems, *Quantum* **5**, 486 (2021).

- [47] M. Grabowski and P. Mathieu, Structure of the conservation laws in quantum integrable spin chains with short range interactions, *Ann. Phys.* **243**, 299 (1995).
- [48] See Supplemental Material at <http://link.aps.org/supplemental/10.1103/PhysRevB.109.L161109> for the discussion of the overlaps of LIOMs, details of numerical calculations, the finite-size effects, dynamics of rotated operators and the energy current, and results for other perturbations and comparison with the Boltzmann equation, which also include Refs. [49–51].
- [49] J. Durnin, M. J. Bhaseen, and B. Doyon, Nonequilibrium dynamics and weakly broken integrability, *Phys. Rev. Lett.* **127**, 130601 (2021).
- [50] L. Bonnes, F. H. L. Essler, and A. M. Läuchli, “Light-cone” dynamics after quantum quenches in spin chains, *Phys. Rev. Lett.* **113**, 187203 (2014).
- [51] M. Takahashi, *Thermodynamics of One-Dimensional Solvable Models* (Cambridge University, Cambridge, England, 1999).
- [52] T. J. Park and J. C. Light, Unitary quantum time evolution by iterative Lanczos reduction, *J. Chem. Phys.* **85**, 5870 (1986).
- [53] M. Mierzejewski and P. Prelovšek, Nonlinear current response of an isolated system of interacting fermions, *Phys. Rev. Lett.* **105**, 186405 (2010).
- [54] C. Bartsch and J. Gemmer, Dynamical typicality of quantum expectation values, *Phys. Rev. Lett.* **102**, 110403 (2009).
- [55] J. Gemmer, M. Michel, and G. Mahler, *Quantum Thermodynamics: Emergence of Thermodynamic Behavior within Composite Quantum Systems*, Lecture Notes in Physics, Vol. 784 (Springer, Berlin, 2009).
- [56] T. A. Elsayed and B. V. Fine, Regression relation for pure quantum states and its implications for efficient computing, *Phys. Rev. Lett.* **110**, 070404 (2013).
- [57] R. Steinigeweg, J. Gemmer, and W. Brenig, Spin-current auto-correlations from single pure-state propagation, *Phys. Rev. Lett.* **112**, 120601 (2014).
- [58] R. Steinigeweg, J. Gemmer, and W. Brenig, Spin and energy currents in integrable and nonintegrable spin- $\frac{1}{2}$  chains: A typicality approach to real-time autocorrelations, *Phys. Rev. B* **91**, 104404 (2015).
- [59] Wrocław Center for Networking and Supercomputing, <http://wcss.pl>.